

Figure W1. (A) Extracted ion chromatogram of sarcosine and alanine in urine. (B) Selected ion monitoring of alanine and sarcosine.

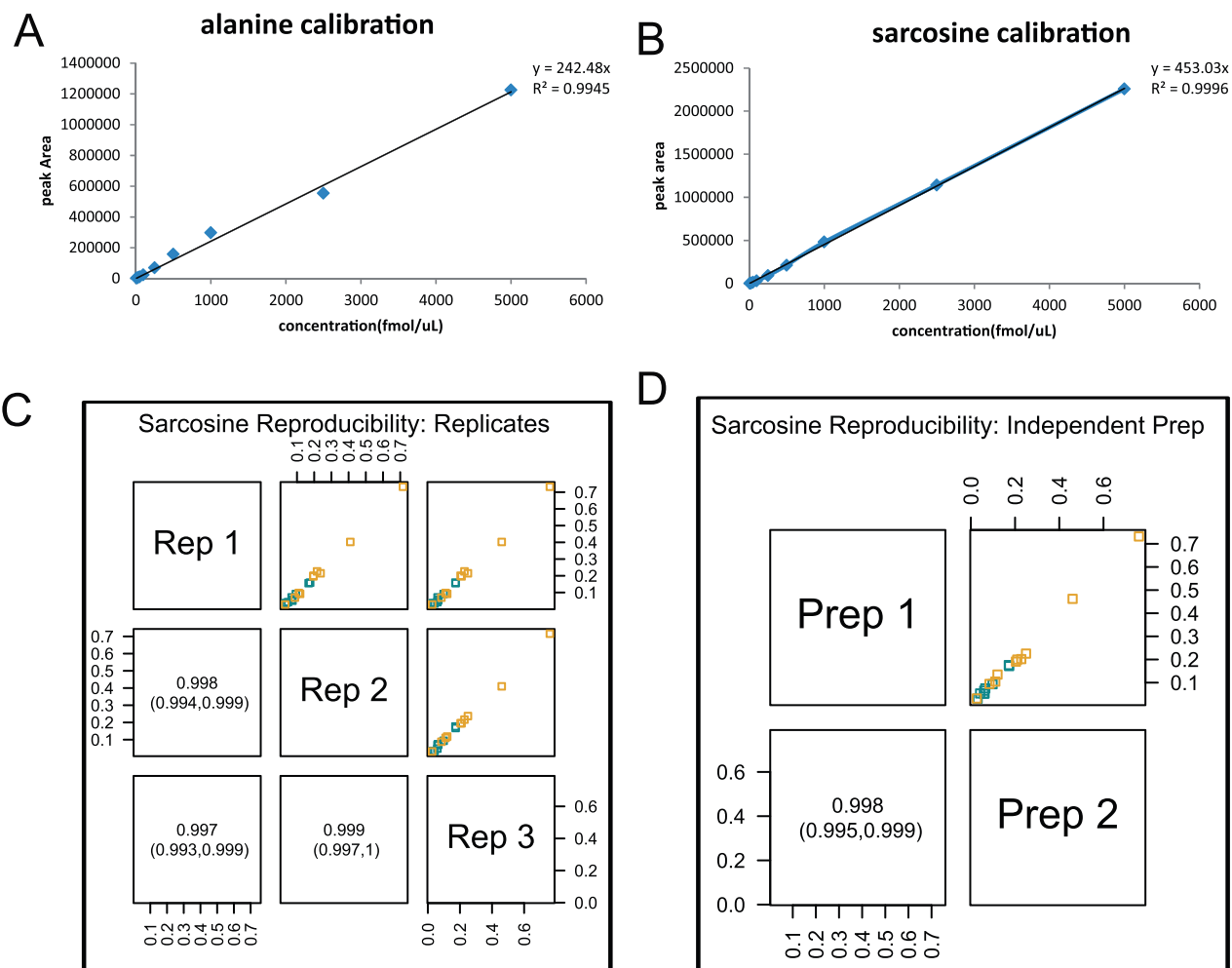


Figure W2. Calibration curve of (A) alanine (B) sarcosine. (C and D) Reproducibility of sarcosine assessment using isotope dilution GC-MS. Sarcosine measurement for 10 biopsy-positive and 10 biopsy-negative urine samples using two independent experiments was highly correlated with $\rho > 0.9$. The horizontal and vertical axes represent the sarcosine/alanine ratio for the corresponding technical replicates (runs 1 and 2) of the urine sediments. Values inside the boxes indicate the correlation (ρ) for the given comparison with the 95% confidence interval (CI) values in parenthesis.

Table W1. Sequence of Gene-Specific PCR Primers Used for Cloning and qPCR.

Gene-Specific Primer	Primer Sequence
<i>Nor1</i> -GNMT F	5'-TTTTCCCTTTGCGGCCGCgtggacagcgtgtaccggacc-3'
<i>EcoRI</i> -GNMT R	5'-CCGGAATTCtcaagtctgtctctttagcac-3'
<i>Nor1</i> -SARDH F	5'-TTTTCCCTTTGCGGCCGCgcctcactgagccgagcccta-3'
<i>XbaI</i> -SARDH R	5'-CTAGTCTAGAtcagtagattcccttcaccct-3'
<i>Nor1</i> -PIPOX F	5'-TTTTCCCTTTGCGGCCGCgaggctcagaagatctctg-3'
<i>XbaI</i> -PIPOX R	5'-CTAGTCTAGActaaagggtggctttgccagget-3'
GNMT F*	5'-CTTCATCCACGTGCTCAAGA-3'
GNMT R*	5'-TCCCCATCTTCCAGACAGAG-3'
SARDH F*	5'-CTGATGAATGTGGACGACCT-3'
SARDH R*	5'-GTTCTCAATGACCTGTGCTC-3'
PIPOX F*	5'-CCTGTCTTTGCTTGCCTTTG-3'
PIPOX R*	5'-GAAGGGACACAGTACCTGCTC-3'

F and R stand for forward and reverse primers respectively.

*Denotes set of primers used for qPCR analysis.

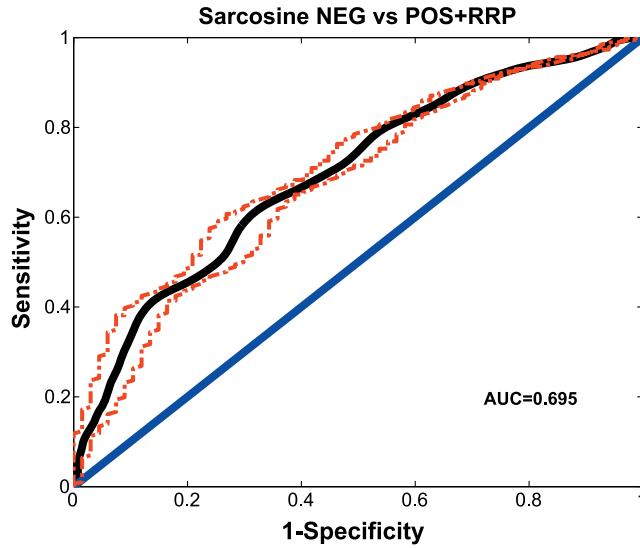


Figure W3. AUROC for sarcosine in the 652 urine sediments from 168 biopsy-negative, 261 biopsy-positive, and 210 RRP individuals was 0.695.

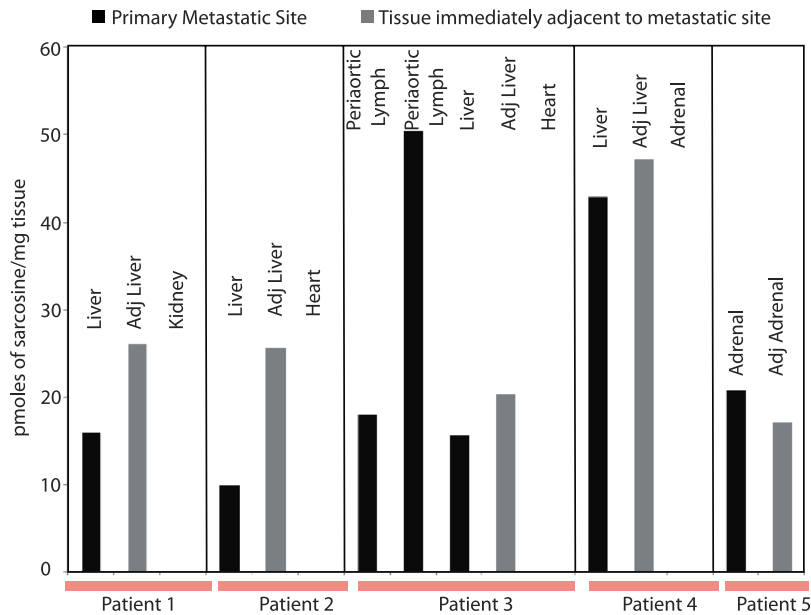


Figure W4. Sarcosine levels in metastatic and benign tissues of five different cancer patients. Sarcosine levels were found to be comparably high in both metastatic tumor (black) and its matched adjacent pathologically benign tissues (gray), while still being undetectable in distal nontumor tissues resected from the same patient [1].

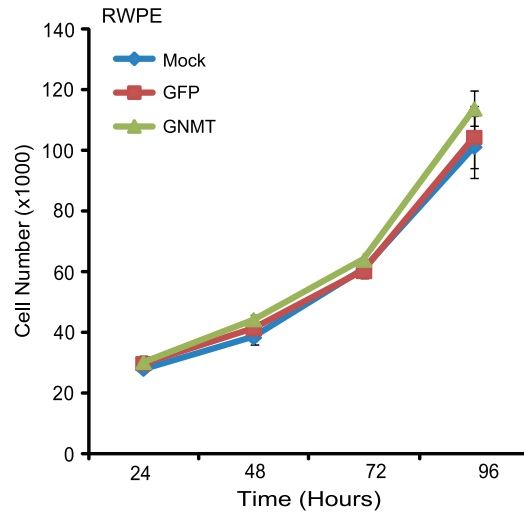


Figure W5. GNMT overexpression does not affect proliferation of benign RWPE prostatic epithelial cells. The benign immortalized prostate cell line RWPE was transduced for overexpression of GNMT or GFP vector control. We observed no significant difference in cell proliferation in RWPE-GNMT overexpressing cells relative to either GFP transduced or mock.

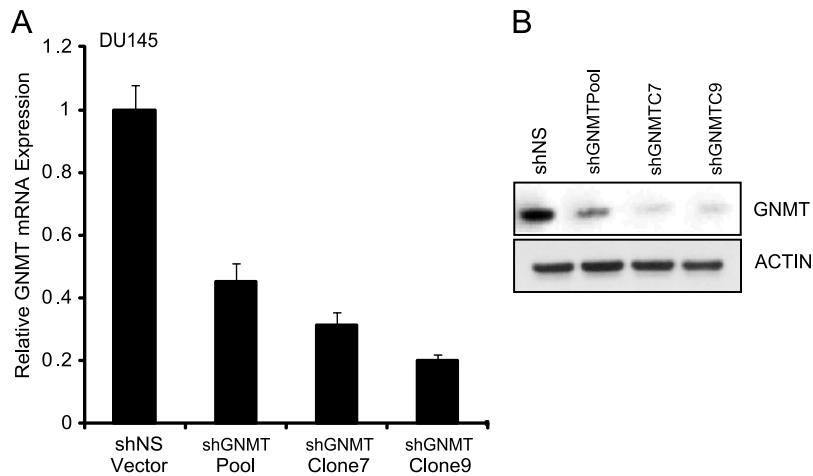


Figure W6. qRT-PCR and immunoblot analysis of GNMT knockdown in DU145 cells. (A) qPCR analysis of GNMT transcript in stable shGNMT knockdown cells (stably selected pool and clones). (B) Western blot analysis showing stably puromycin-selected clones of GNMT knockdown in DU145 cell model.

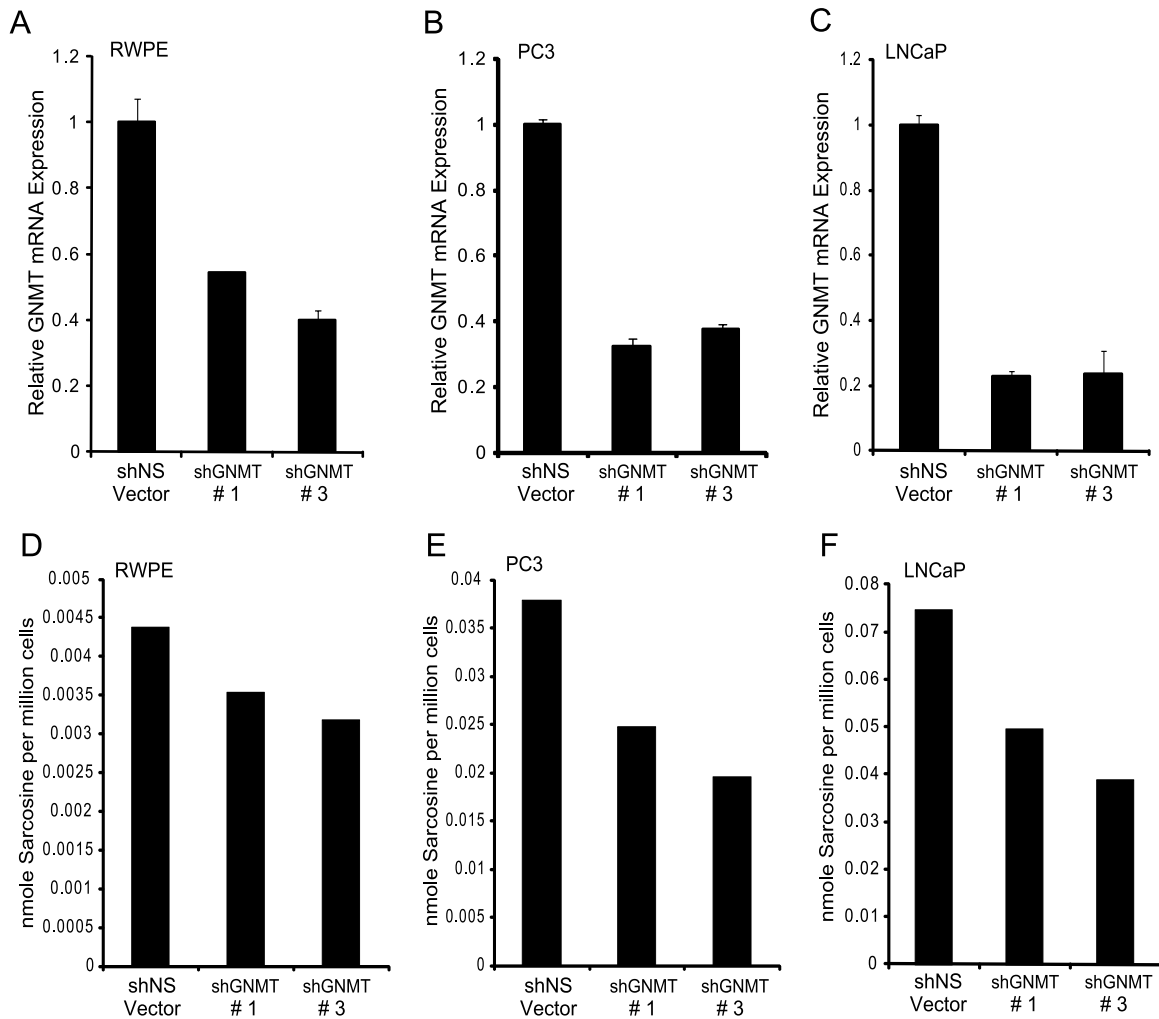


Figure W7. Validation of GNMT knockdown followed by assessment of sarcosine levels in RWPE, PC3, and LNCaP cells. qPCR analysis of GNMT transcript in stable shGNMT knockdown (A) RWPE, (B) PC3, and (C) LNCaP cells. Sarcosine levels were assessed by GC-MS in stable shGNMT knockdown (D) RWPE, (E) PC3, and (F) LNCaP cells. We observed significant decrease in sarcosine levels after stable GNMT knockdown in PC3 and LNCaP cells.

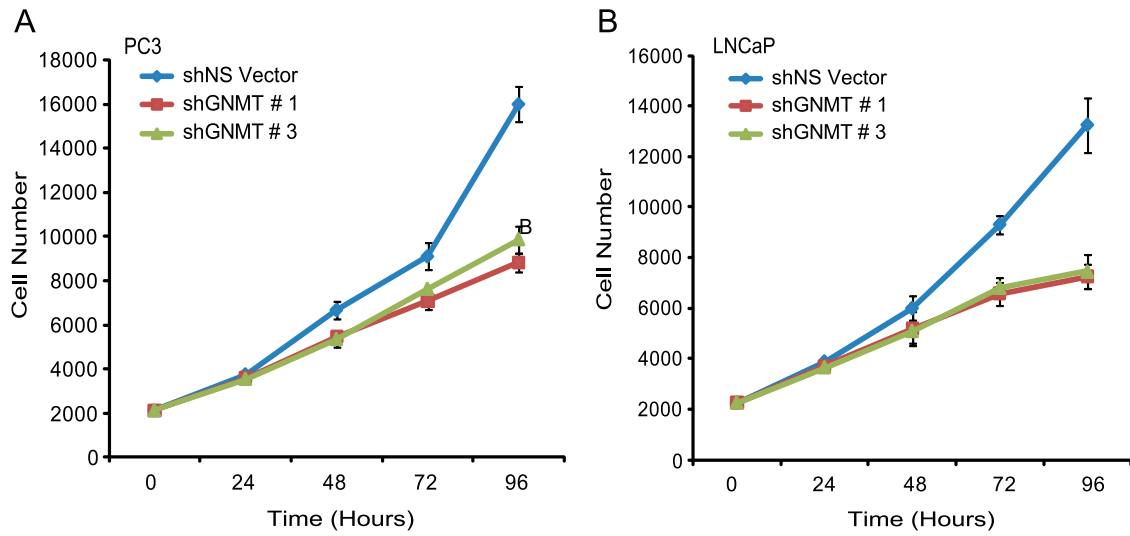


Figure W8. GNMT knockdown decreases cell proliferation in (A) PC3 and (B) LNCaP cells. GNMT knockdown in metastatic prostate carcinoma (PC3) and androgen-responsive (LNCaP) cells resulted in the significant decrease in cell proliferation.

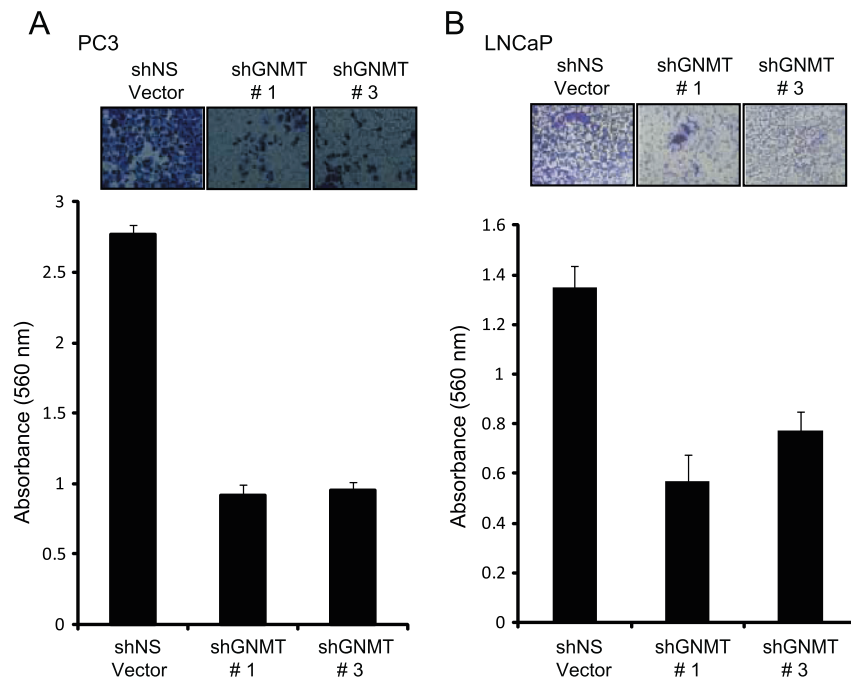


Figure W9. GNMT knockdown attenuates invasion in PC3 and LNCaP cells. (A) PC3 and (B) LNCaP cells were transduced with shGNMT, or shNS vector control, stable cells were generated and assayed for cell invasion.

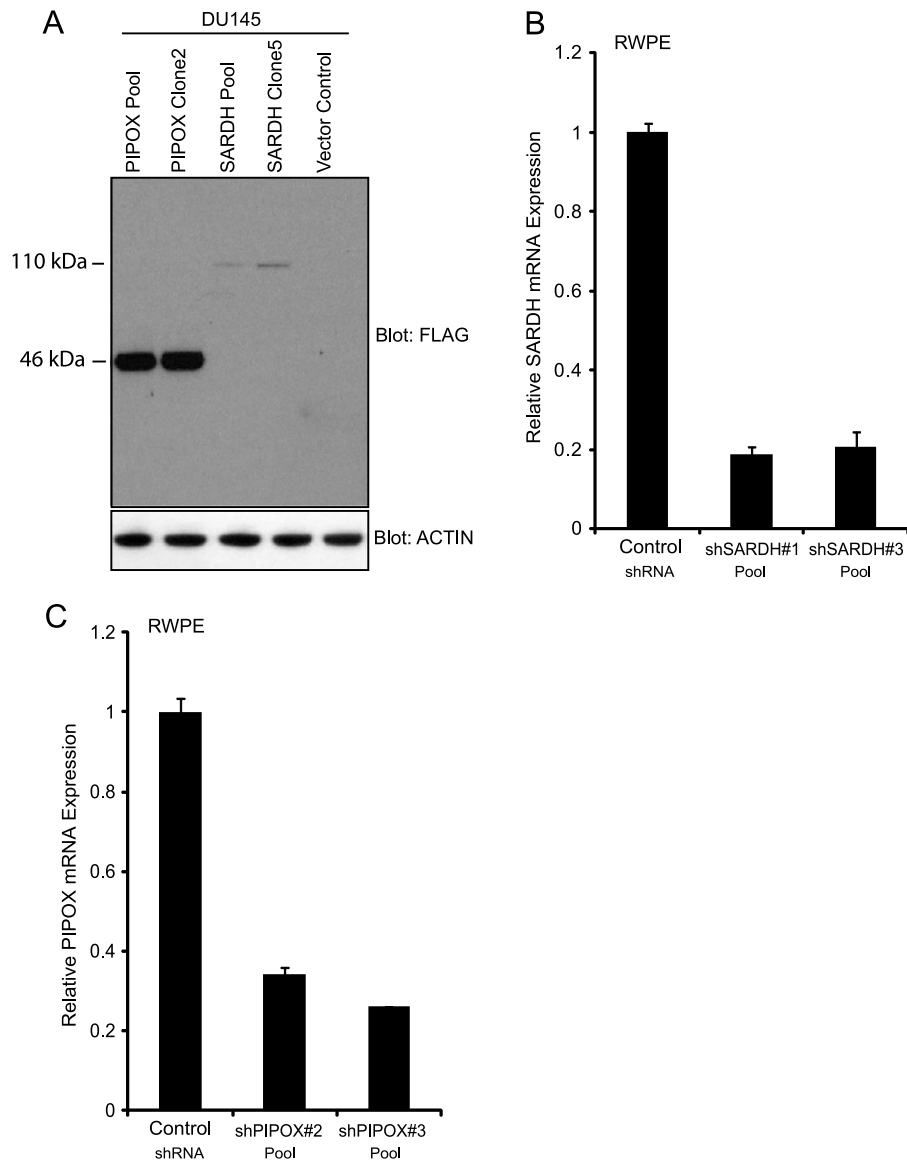


Figure W10. Validation of overexpression and knockdown of SARDH and PIPOX in DU145 and RWPE cells, respectively. (A) Western blot showing stably transfected FLAG-tagged PIPOX and FLAG-tagged SARDH expression (pool and clones; DU145 cells). Actin was used as loading control. qPCR analysis of RNA isolated in parallel to the invasion assay of (B) SARDH and (C) PIPOX.

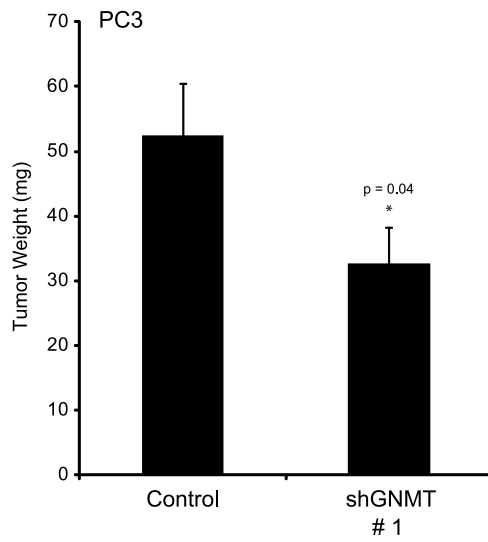


Figure W11. Tumor weight decreases in GNMT knockdown PC3 xenografts in CAM assay compared to vector control.

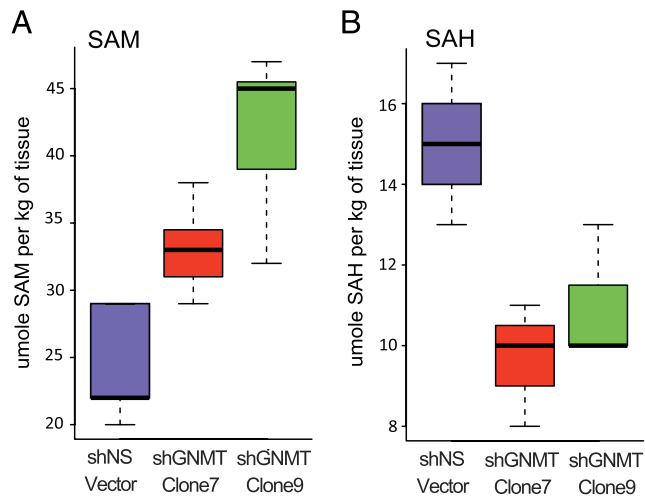


Figure W12. Assessment of SAM and SAH in GNMT knockdown mouse xenograft. (A) Box plot of SAM. (B) Box plot of SAH.